Efficient Photoluminescence and Electroluminescence from Environmentally Stable Polymer/Clay Nanocomposites

Tae-Woo Lee,[†] O O. Park,*[,†] Jang-Joo Kim,[‡] Jae-Min Hong,[§] and Young C. Kim

Center for Advanced Functional Polymers and Department of Chemical Engineering, Korea Advanced Institute of Science and Technology, 373-1, Kusong, Yusong, Taejon 305-701, Korea, Department of Material Science and Technology, Kwangju Institute of Science and Technology, 1, Oryong-dong, Buk-gu, Kwangju 500-712, Korea, and Polymer Materials Laboratory, Korea Institute of Science and Technology, P.O. Box 131, Cheongryang, Seoul 130-650, Korea

Received March 8, 2001

The potential use of polymer light-emitting devices is ultimately limited by their low quantum efficiency as well as by their poor stability against oxygen and moisture. To simultaneously solve these drawbacks, light-emitting devices using the polymer/layered silicate nanocomposite with good gas-barrier properties were fabricated by blending poly-[2-methoxy-5-(2′-ethyl-hexyloxy)-1,4-phenylenevinylene] (MEH-PPV) with organoclay. The 2-dimensional nanocomposite film shows higher photoluminescence (PL) output and better photostability when compared with the pure MEH-PPV film of the same thickness. Electroluminescence (EL) efficiency is also enhanced. This 2-dimensional lamellar type nanocomposite structure efficiently confines not only both electrons and holes to enhance the recombination rate but also excitons to improve singlet radiative decay. By analyzing transient EL behavior, it was found that the charge carrier mobility of the nanocomposite device was reduced, which suggests that effective charge blocking improves the bipolar recombination rates. Additionally, the isolation of polymer chains within a confined geometry by intercalation prevents excitons from finding low-energy trap sites. Therefore, PL and EL quantum yield is improved.

Introduction

Since electroluminescence (EL) from (*p*-phenylene vinylene) (PPV) was discovered in 1990, polymer light-emitting diodes (LEDs) have been considered promising candidates for flat, large-area displays.[1,2] The polymer light-emitting device is receiving considerable attention due to easy fabrication with low cost, low operating voltage, color variability, mechanical flexibility, and so forth. However, commercial use of the EL devices is ultimately limited by their low quantum efficiency as well as by their poor stability against oxygen and moisture. Therefore, a lot of research has been focused on solving the problems.[3−8] In the case of LEDs made of p-type polymers such as PPV derivatives, poly(*p*-phenylene)s, polyfluorenes, and polythiophenes, the majority of the carriers of the emissive polymers are holes. Therefore, one of the major reasons for the low quantum efficiency of single-layer LEDs is that the electron injection current is too low.[3,4] To make a more efficient electroluminescent device, it is necessary to enhance the injection and confinement of the charge carriers. To improve the electron injection properties, several methods in device design and fabrication have been reported: (i) use of a cathode with a low work function,[3] (ii) use of an electron-injecting or -transporting layer,[5,6] (iii) use of an insulating layer such as Al_2O_3 to reduce the effective energy barrier,[7] and (iv) post-deposition annealing above the glass transition temperature of an emitting polymer for the purpose of enhancement of the interfacial adhesion between an emitting layer and a metal electrode.[8] Approaches to improve the luminescent efficiency by molecular engineering have been tried, which are to promote the electron injection ability by attaching a moiety with high electron affinity to emissive backbones[9] or to enhance the exciton confinement by alternative arrangement of conjugated and nonconjugated segments with surrounding side groups for chromophores.[10] A quantum-well

* To whom correspondence should be addressed.
[†] Korea Advanced Institute of Science and Technology.
[‡] Kwangju Institute of Science and Technology.
[§] Korea Institute of Science and Technology.

(1) Burroughes, J. H.; Bradley, D. D. C.; Brown, A. R.; Marks, R. N.; Mackay, K.; Friend, R. H.; Burns, P. L.; Holmes, A. B. *Nature* **1990**, *347*, 539.
(2) Braun, D.; Heeger, A. J. *Appl. Phys. Lett.* **1991**, *58*, 1982.
(3) Parker, I. D. *J. Appl. Phys.* **1994**, *75*, 1659.
(4) Jenekhe, S. A.; Zhang, X.; Chen, X. L.; Choong, V. E.; Gao, Y.; Hsieh, B. R. *Chem. Mater.* **1997**, *9*, 409.
(5) O'Brien, D.; Weaver, M. S.; Lidzey, D. G.; Bradley, D. D. C. *Appl. Phys. Lett.* **1996**, *69*, 881.
(6) Lee, T.-W.; Park, O. O. *Appl. Phys. Lett.* **2000**, *76*, 3161.
(7) Li, F.; Tang, H.; Anderegg, J.; Shinar, J. *Appl. Phys. Lett.* **1997**, *70*, 1233.
(8) Lee, T.-W.; Park, O. O. *Adv. Mater.* **2000**, *12*, 801.
(9) Chung, S.-J.; Kwon, K.-Y.; Lee, S.-W.; Jin, J.-I.; Lee, C.-H.; Lee, C. E.; Park, Y. *Adv. Mater.* **1998**, *10*, 1112.
(10) Sun, R. G.; Wang, Y. Z.; Wang, D. K.; Zheng, Q. B.; Kyllo, E. M.; Gustafson, T. L.; Epstein, A. J. *Appl. Phys. Lett.* **2000**, *76*, 634.

10.1021/cm010201h CCC: $20.00
Published on Web 05/23/2001

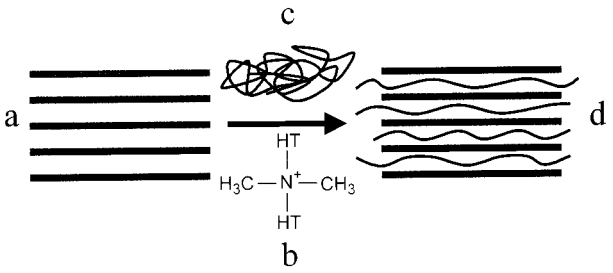

Figure 1. Schematic diagram of the intercalation process: (a) native clay; (b) inorganic charge exchange cation (CEC) (dimethyl dihydrogenated-tallow (HT) ammonium); (c) MEH-PPV; (d) 2-dimensional morphology of the intercalated composite. The native clay material possesses an anionic character (OH^-). The CEC is needed to compatibilize the hydrophobic polymer and inorganic clay.

structure for the charge confinement was also employed to improve the electron−hole recombination rate of the organic EL device.[11] However, it is not easy to fabricate the multilayer device by successive spin-casting of polymer solutions. The improvement of device stability is more urgently required to commercialize the polymeric EL device. Conjugated polymers used in polymer LEDs are inherently susceptible to oxygen and moisture. One generally understood way to improve the stability is to prevent oxygen and moisture from penetrating into the emissive layer, for example, by using a polyaniline buffer layer on the top of an indium tin oxide (ITO) anode[12] or by using an environmentally stable cathode such as Al. Design of novel organic/inorganic composite materials with 2-dimensional geometry can be a fundamental solution to greatly improve the environmental stability.

In this work, nanostructured composite materials consisting of conjugated polymers and layered inorganic silicas are the focus of interest due to their novel physical, electronic, and optical properties. Recently, nanocomposites of polymer with layered silicate have been studied by many researchers.[13−17] We used conjugated polymer/layered silicate nanocomposite material for the EL device to simultaneously improve the EL efficiency and the stability against oxygen and moisture. The layered silicate is a 2-dimensional layer-structured material as shown in Figure 1a and possesses a good physical property to overcome the environmental instability of conjugated polymers: a good gas-barrier property due to its lamellar-type layered physical structure.[13] Layered silicates dispersed in a polymer matrix are known as one of the most interesting forms of hybrid organic−inorganic nanocomposites.[14] The nanolayers are of preferred face-to-face stacking in agglomerated tactoids, and there exists an intrinsic incompatibility between hydrophilic layered silicates and typical hydrophobic polymers. Thus, dispersion of the tactoids into discrete monolayers is not an easy process. The replacement of the inorganic charge exchange cations in the galleries of the native clay by dimethyl dihydrogenated-tallow (HT[18]) ammonium (Figure 1b) surfactants is known to compatibilize the surface chemistry of the clay and the hydrophobic polymer.[19] Such replacement can serve not only to match the polarity of the clay surface with that of polymers (Figure 1c) but also to expand the clay galleries. This facilitates the penetration of the polymer precursors or preformed polymer into the gallery space (intercalation). The intercalated structure schematically looks like Figure 1d. The conjugated and conducting nanostructures in porous zeolite were studied by Bein,[20] and the insertion of PPV by intercalating the PPV precursor polymer between the layers of MoO_3 was also reported.[21] In this work, we tried intercalation of a conjugated polymer into layered silicate such as montmorillonite and fabricated EL devices based on the layered nanocomposite. When a conjugated polymer/organoclay nanocomposite is employed for an EL device, we expect an electronic structure similar to a well-known quantum well in a small nanodomain; thus, good charge confinement in the structure can be achieved. Although Carter and co-workers have fabricated nanocomposite polymer LEDs using sphere-shape nanoparticles such as SiO_2 and TiO_2,[22,23] they did not intended to improve the charge confinement and the environmental stability as we did. Recently, several papers reported the effect of polymer morphology on the luminescent efficiency;[24−27] theses works also reported strong dependence of optical properties of conjugated polymers on chain conformation, which opens room for the use of nanoscale architecture to control the polymer conformation. In particular, isolation of conjugated polymer chains within inorganic materials plays an important role in improving the luminescent efficiency and controlling interchain energy transfer.[27] In this paper, we studied the effect of intercalation (or isolation within 2-dimensional geometry) of an emitting polymer into organoclay on the efficiency and stability of photoluminescence (PL) and EL.

Experimental Section

Materials. We synthesized the emitting polymeric material, poly[2-methoxy-5-(2′-ethylhexyloxy)-1,4-phenylenevinylene] (MEH-PPV), according to the reported synthesis scheme.[28] An organically modified mica-type silicate (C6A) by dimethyl HT ammonium with the charge exchange capacity of 140 mequiv/100 g was purchased from Southern Clay Product Inc. (Gonzales, TX) and sonicated in 1,2-dichloroethane solvent for 3 h

(11) An, H. Y.; Chen, B. J.; Hou, J. Y.; Shen, J. C.; Liu, S. Y. *J. Phys. D* **1998**, *31*, 1144.
(12) Karg, S.; Scott, J. C.; Salem, J. R.; Angelopoulos, M. *Synth. Met.* **1996**, *80*, 111.
(13) Yano, K.; Usuki, A.; Okada, A.; Kurauchi, T.; Kamigito, O. *J. Polym. Sci.: Part A* **1993**, *31*, 2493.
(14) Okada, A.; Usuki, A. *Mater. Sci. Eng. C* **1995**, *3*, 109.
(15) Bujdák, J.; Hackett, E.; Cignnelis, P. *Chem. Mater.* **2000**, *12*, 2168.
(16) Kawashima, D.; Aihara T.; Kobayashi, Y.; Kyotani, T.; Tomita, A. *Chem. Mater.* **2000**, *12*, 3397.
(17) Kim, D. W.; Blumstein, A.; Kumar, J.; Tripathy, S. K. *Chem. Mater.* **2001**, *13*, 243.
(18) Dihydrogenated-tallow (HT) is predominantly an octadecyl chain with smaller amounts of lower homologues (approximate composition: C18, ∼65%; C16, ∼30%; C14, ∼15%).
(19) Fukushima, Y.; Inagaki, S. *J. Inclusion Phenom.* **1987**, *5*, 473.
(20) Bein, T. *Stud. Surf. Sci. Catal.* **1996**, *102*, 295.
(21) Nazar, L. F.; Zhang, Z.; Zinkweg, D. *J. Am. Chem. Soc.* **1992**, *114*, 6239.
(22) Bliznyuk, V.; Ruhstaller, B.; Brock, P. J.; Sherf, U.; Carter, S. A. *Adv. Mater.* **1999**, *11*, 1257.
(23) Carter, S. A.; Scott, J. C.; Brock, P. J. *Appl. Phys. Lett.* **1997**, *71*, 1145.
(24) Jenekhe, S. A.; Osaheni, J. A. *Science* **1994**, *265*, 765.
(25) Shi, Y.; Liu, J.; Yang, Y. *J. Appl. Phys.* **2000**, *87*, 4254.
(26) Nguyen, T.-Q.; Martini, I. B.; Liu, J.; Schwartz, B. J. *J. Phys. Chem. B* **2000**, *104*, 237.
(27) Nguyen, T.-Q.; Wu, J.; Doan, W.; Schwartz, B. J.; Tolbert, S. H. *Science* **2000**, *288*, 652.
(28) Heeger, A. J.; Braun, D. (UNIAX) **1992,** WO-B 92/16023; *Chem. Abstr.* **1993**, *118*, 157401j.

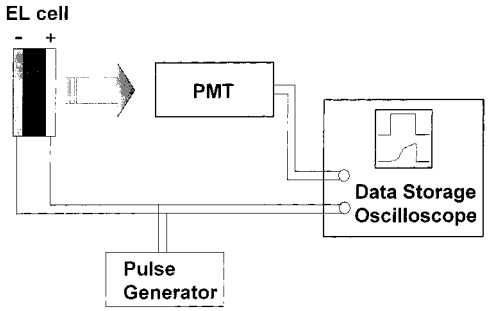

Figure 2. Experimental setup used to measure the transient EL behaviors of the devices.

for good dispersion before use. MEH-PPV was dissolved in 1,2-dicholoethane by stirring for 6 h. Each solution was mixed and then sonicated for 2 more hours and then stirred for an additional 3 h. The weight ratios of MEH-PPV versus C6A were changed from 5:1 to 1:1, and we denoted MEH-PPV/clay (5:1 by wt, 16.7 wt % of clay), MEH-PPV/clay (2:1 by wt, 33.3 wt % of clay), and MEH-PPV/clay (1:1 by wt, 50 wt % of clay) as MEH5/clay1, MEH2/clay1, and MEH1/clay1, respectively.

Device Fabrication. Single-layer polymer light-emitting devices of pure MEH-PPV and the MEH-PPV/C6A composite were fabricated as follows: 120 nm thick emitting films were spin-cast from the 1,2-dichloroethane solutions on indium tin oxide (ITO)-coated glass substrates. Upon application of shear force parallel to the ITO glass by spin-casting, the clay with large aspect ratios (500−1000) in the composite solution could be aligned along the substrate. Baking of the spin-coated thin films was done at 100 °C in a vacuum oven. And Al as a cathode was deposited under a high vacuum (1×10^{-6} Torr).

Measurement of Electrical and Luminescent Properties. The electrical and luminescent characteristics of the devices were measured by using a current/voltage source-measurement unit (Keithley 236), a spectroradiometer (Minolta CS-1000), and an optical power meter (Newport 835). EL and photoluminescence (PL) spectra were measured using a dual grating monochromator (Spex 270M) with the photomultiplier tube (PMT) (Hamamatsu R928) as a detector.

Transient EL Measurement. We measured transient EL of LED devices by the setup illustrated in Figure 2. EL cells were operated by a pulse generator (HP 214B), which was also externally triggered by a function generator (Phillips PM 5139) at a low frequency of 10 Hz. EL was detected by a fast PMT (Hamamatsu Photonics R928, whose response time was 2.2 ns). The transient behavior of the EL was measured with a fast storage oscilloscope (HP Infinium). The voltage pulse was also observed with the storage oscilloscope at the same time.

Results and Discussion

XRD Characteristics. To confirm the intercalation of MEH-PPV into the gallery of C6A, an X-ray diffraction (XRD) study was carried out. Figure 3 shows the XRD curves of the bulk organoclay and the MEH/clay composite films, whose peaks are found at $2\theta = 2.65$ and 2.35°, respectively. Three composite films show a practically identical XRD peak position regardless of the blend ratio. The peaks are attributed to the Bragg diffraction from the 001-lattice planes of C6A. Interlay d_{001}-spacings are expanded from 33.3 Å in pure C6A to 37.6 Å in a MEH-PPV/C6A composite film by the intercalation of MEH-PPV molecules into the gallery of C6A. Therefore, MEH-PPV is isolated within the 2-dimensional lamellar structure. As the clay composition increases, the portion of isolated MEH-PPV within the gallery of clay increases. The coiled chain structure (Figure 1c) of MEH-PPV could be stretched out within the 2-dimensional confined geometry (Figure 1d). In this case, we can expect a huge decrease of interchain

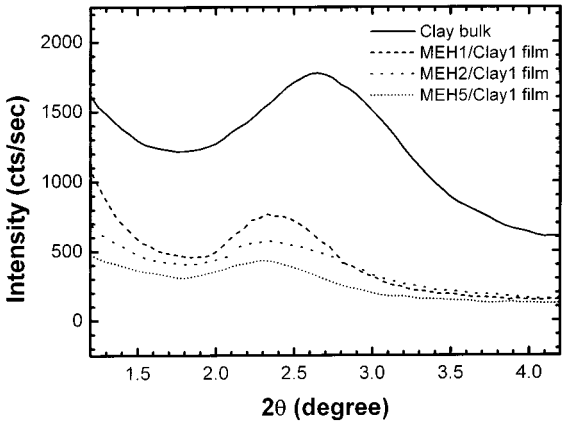

Figure 3. XRD curves of organoclay (C6A) bulk and MEH-PPV/C6A nanocomposite films with several different blend ratios.

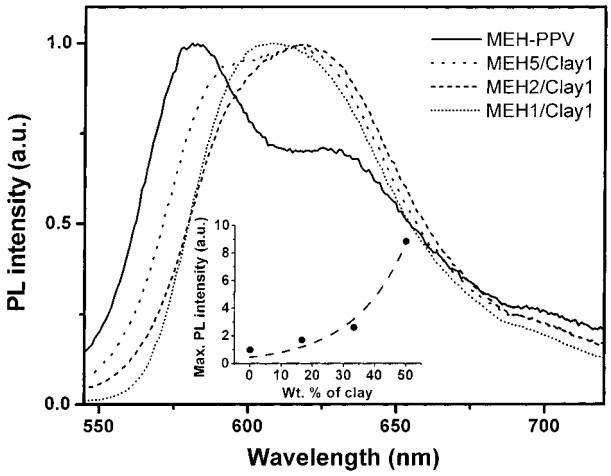

Figure 4. Normalized PL intensity of the MEH-PPV/clay nanocomposites with several different blend ratios. The inset shows the maximum PL intensity of the materials increases with an increase of the clay composition.

interaction. The degree of interchain interaction strongly affects the PL spectra and quantum yield.[24,27,29−31] Therefore, it is important to reduce the interchain interaction to improve the PL quantum yield.

PL Characteristics. Figure 4 shows the normalized PL spectra of the MEH-PPV/C6A composite films of the same thickness. The excitation at 500 nm was performed at a 45° angle of the thin film plane. The emission was detected at a right angle with respect to the excitation beam direction. The UV/vis absorption spectra of the composite films with the same thickness were used to confirm that the composition of MEH-PPV decreases as that of C6A increases. The PL spectra of the composite films are red-shifted, and the line width tends to decrease as the clay composition increases. We attribute this feature to an intercalation-induced conformational transition from compact coil (Figure 1c) to extended coil (Figure 1d). When the polymer chains were intercalated in the 2-dimensional confined geometry, the effective conjugation length would increase due

(29) Yan, M.; Rothberg, L. J.; Papadimitrakopoulos, F.; Galvin, M. E.; Miller, T. M. *Phys. Rev. Lett.* **1994**, *73*, 744.
(30) Yan, M.; Rothberg, L. J.; Kwock, E. W.; Miller, T. M. *Phys. Rev. Lett.* **1995**, *75*, 1992.
(31) Jakubiak, R.; Rothberg, L. J.; Wan, W.; Hsieh, B. R. *Synth. Met.* **1999**, *101*, 230.

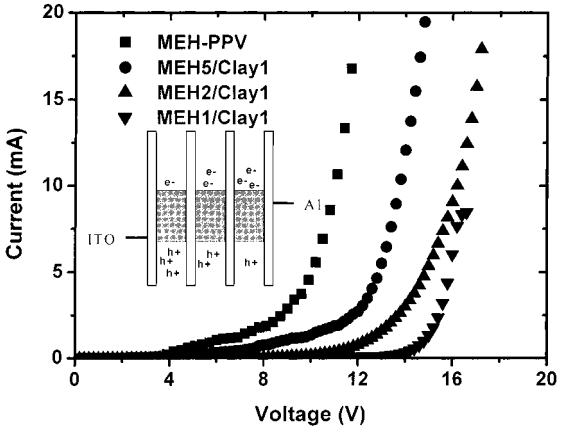

Figure 5. Current versus voltage characteristics of ITO/(MEH-PPV/clay nanocomposite)/Al devices with several different blend ratios. The inset shows the schematic band energy diagram of the composite EL devices in the nanodomain. The device could form a quantum-well-like structure for a good quantum confinement.

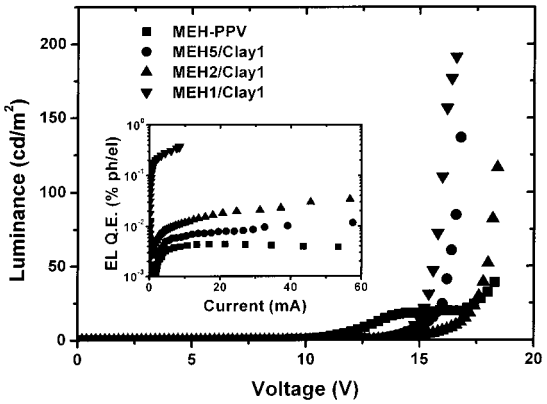

Figure 6. Luminance versus voltage characteristics of ITO/(MEH-PPV/clay nanocomposite material)/Al devices with several different blend ratios. The inset shows the EL quantum efficiency of the nanocomposite material devices with an Al electrode.

to the chain planarization. In addition, the interchain Förster energy transfer is difficult. Instead, intrachain energy transfer would take place dominantly. Therefore, the higher energy excitons would migrate into the lower energy state along the single chain, resulting in a spectral red-shift. Luminescent color tuning by adjusting the length of π-conjugated segments has been reported previously.[32] The intercalation process could also provide an additional means to shift the emission color by changing the effective conjugation length. The MEH-PPV/C6A composite materials also exhibit a peculiar PL behavior: the enhancement of photoluminescence (PL) although there is a reduction of the emitting MEH-PPV composition. The PL intensity was greatly enhanced (9 times higher than that of the pure MEH-PPV film with the same thickness or 18 times if we consider the reduced amount ($^1/_2$) of MEH-PPV) as demonstrated in the inset of Figure 4. We attribute this phenomenon to the following two reasons: The first is huge reduction of interchain interaction. The effect of interchain interactions in conjugated polymers on PL quantum yield has been reported by several researchers.[24−27,29−31] Isolating the conjugated polymer chains within a confined geometry prevents excitons from finding low-energy trap sites. Therefore, improvement of PL quantum yield can be achieved. The second possibility is the increase of effective excitation energy due to an increased excitation beam path by internal scattering or reflection within the composite film which could be induced by the refractive index difference between MEH-PPV and the intercalated tactoids. The internal scattering may also lead to a reduction of PL loss by preventing the waveguide within the film. From these two reasons, we may obtain dramatically improved PL output.

Electrical and Luminescent Properties of the LEDs. Figure 5 shows the current versus voltage characteristics of the MEH/C6A nanocomposite light-emitting diodes. The current tends to decrease with increasing composition of C6A, which means that it blocks the flow of electrons and holes. Because they are isolated within a 2-dimensional confined geometry, hopping between the polymer chains is difficult. Electrons and holes could be effectively confined in the quantum-well-like structure as schematically illustrated in the inset of Figure 5. Thus, the probability of exciton formation by bipolar recombination will increase. In addition, the produced excitons can also be confined effectively within the narrow geometry and perform singlet decay efficiently before losing the energy via a nonradiative decay. As a result, the EL efficiency drastically increases as shown in the inset of Figure 6. Figure 6 shows the luminance versus voltage characteristics of our devices. The nanocomposite device shows enhanced luminance compared with that of the pure MEH-PPV single-layer device. As clay composition increases, the luminance also tends to increase; this tendency agrees well with the PL output as shown in Figure 4. The external EL quantum efficiencies were measured by using a procedure similar to those reported previously.[33] The external quantum efficiency of the pure MEH-PPV single-layer device was determined as 4×10^{-3} % photons/electrons, which is close to the values reported elsewhere.[3,34] But our MEH-PPV device demonstrated high stability under high electric field, so that the maximum luminance is relatively higher than the reported value elsewhere.[34] The ITO/(MEH1/clay1)/Al device showed an improved external quantum efficiency, 0.38% photons/electrons (~100 times enhanced). As clay composition increases, the luminance at the same current increases because of a more effective confinement of charges and excitons. For instance, the luminance of the MEH1/clay1 blend device at 8.5 mA reaches 192 cd/m^2, while that of the pure MEH-PPV device at the same current is only 2 cd/m^2. Additionally, the onset voltage for light emission of the MEH1/clay1 device was as low as 4 V even though the material was blended with a large portion of the insulating clay. However, there still remains plenty of room for further improvement in device performance. The design and fabrication of novel devices using layered silicate nano-

(32) Malliaras, G. G.; Herrema, J. K.; Wildeman, J.; Wieringa, R. H.; Gill, R. E.; Lampoura, S.; Hadziioannou, G. *Adv. Mater.* **1993**, *5*, 721.

(33) Greenham, N. C.; Friend, R. H.; Bradley, D. D. C. *Adv. Mater.* **1994**, *6*, 491.

(34) Cao, Y.; Yu, G.; Heeger, A. J. *Adv. Mater.* **1998**, *10*, 917.

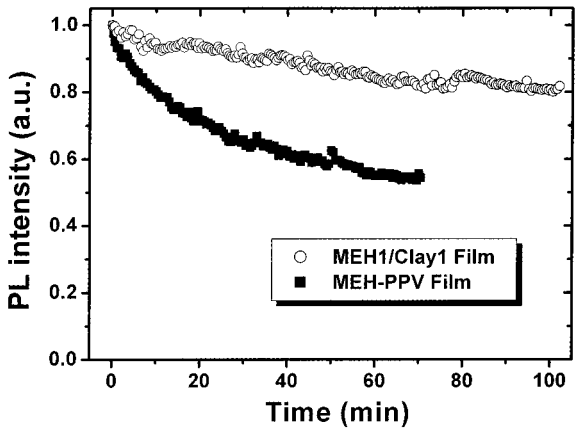

Figure 7. PL intensity of the pure MEH-PPV film and the MEH1/clay1 nanocomposite film spin-cast on glass as a function of the excitation time in air. A strong monochromic 375 nm light from a Xenon lamp was used to excite the films.

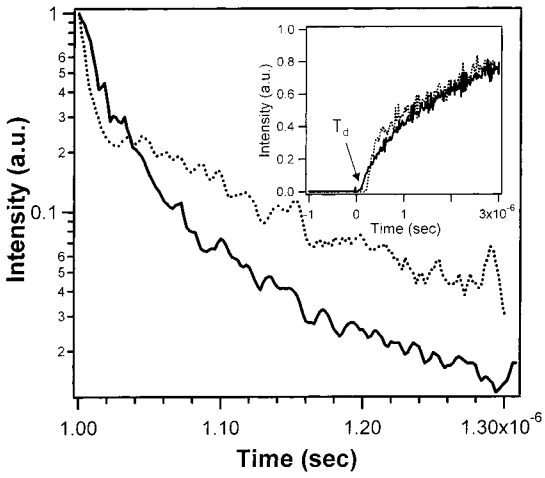

Figure 8. Normalized transient behavior of the EL output from ITO/MEH-PPV/Al (solid line) and ITO/(MEH1/clay1)/Al (dotted line) devices.

composites is in progress. On the other hand, Cao et al. reported that the performance of LEDs can be enhanced by blending the EL polymer with a specific class of surfactant molecules.[34] In our device an ionic surfactant, a dimethyl HT ammonium was incorporated to compatibilize the EL polymer with the native clay. However, the surfactant molecule within our composite material is different from that of Cao's in that it does not have long ethylene oxide chains to enhance the solvation of ions and the complexation with the Al cathode. In Cao's works, the blending of the surfactant molecules without ethylene oxide units with the EL polymer did not contribute to the enhancement of quantum efficiency. Therefore, we believe that the ionic surfactant within the clay gallery does not have a major effect on the enhancement of external EL quantum efficiency.

Photostability Test. Figure 7 shows the change of PL intensity of the MEH1/clay1 composite and the pure MEH-PPV film as a function of time while exciting with the strong monochromatic 375 nm light of a Xenon lamp in air. The PL intensity of the composite film tends to decrease more slowly with time than that of the pure MEH-PPV film. This implies that excitons within the composite possess lower nonradiative decay probability than the pure MEH-PPV film because they are confined so that the hopping to low-energy trapping sites would be largely reduced. When oxygen resides in the films, it accelerates the photooxidation and photodegradation, resulting in a poor quantum efficiency.[29] The composite film, which possesses better environmental stability against oxygen and so forth, will follow a slower photodegradation process.

Transient EL Behaviors. The inset of Figure 8 shows the normalized transient behavior of the EL output from the ITO/MEH-PPV/Al and the ITO/(MEH1/clay1)/Al devices when driven by a pulsed voltage source (1.7×10^8 V/m, 2.6×10^8 V/m, respectively). Previously, we mentioned that the flow of the charge carrier tends to be blocked by the insulating clay layers as shown in Figure 5. To prove this, we observed the transient EL behaviors of the two devices. The mobility was calculated according to the equation $\mu = D/(T_dF)$ (μ = mobility, D = thickness of the emitting layer, T_d = hole transit time, F = electric field) as reported by Hosokawa et al.[35] The T_d was determined from the onset point of EL on the linear-scale graph of Figure 8. The T_d decreases as the applied electric field increases. However, the EL decay profile did not depend on the applied field as previously reported by Hosokawa et al.[35] The EL decay after turning off the device is nonexponential, but it can be described as the sum of two exponential decays. The fast component of the EL decay signal can well be fitted closely to an exponential decay curve. Figure 8 obviously shows that the EL decay rate of the ITO/(MEH1/clay1)/Al device is slower than that of the ITO/MEH-PPV/Al device. The decay rates of the fast components of the two devices are similar (or the decay of the nanocomposite device is slightly faster) until the initial ~20% decay range, but after that, the decay rate of the nanocomposite device is obviously slower. Recently, Nguyen et al. suggested that energy migration along the conjugated polymer backbone (intrachain migration) occurs more slowly than Förster energy transfer between polymer chains (interchain migration).[27] Therefore, they assigned the origin of the fast component of the ultrafast stimulated emission anisotropy decay to the interchain exciton migration and that of the slow component to the intrachain exciton migration. If we discuss the phenomena from Nguyen and her co-workers' viewpoint, the slower decay of the EL signal of the device may originate from the slow intrachain exciton migration because the interchain exciton migration within the MEH1/clay1 composite is very restricted, like the case where Nguyen et al. confined the MEH-PPV chains within the mesoporous silica. In such a case, excitons would not be able to migrate a significant distance along the backbone during its lifetime, reducing the probability of quenching at defect sites so that highly improved PL and EL quantum efficiency can be achieved. However, we are not sure that there is an analogy between the PL decay and EL decay because the measurement time scale is different and the excitons in the EL device exist within a different environment from that of the simply photoexcited films. Specifically, for the EL device, the space charges may influence the recombination process. In the case of the nanocomposite

(35) Hosokawa, C.; Tokailin, H.; Higashi, H.; Kusumoto, T. *Appl. Phys. Lett.* **1992**, *60*, 1220.

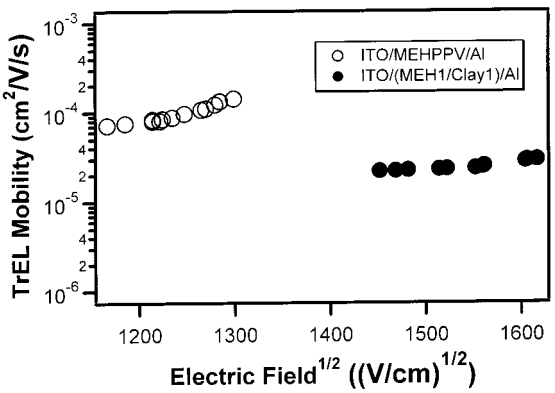

Figure 9. Hole mobilities of the two devices determined by transient EL experiments as a function of electric field strength: ITO/MEH-PPV/Al and ITO/(MEH1/clay1)/Al.

device, the clay blocks the electronic charges within the above-mentioned quantum-well-like structure so that space charges can be formed more than in the ITO/MEH-PPV/Al device. After the device turnoff, the remaining space charges may be recombined to produce light. Therefore, slower decay of the nanocomposite EL device may be possible.

Figure 9 clearly shows that the hole mobility of the device was reduced when the composite was used as an emitting material. The hole mobility of the ITO/MEH-PPV/Al device was $\sim 1 \times 10^{-4}$ cm^2 V^{-1} s^{-1}, while that of the ITO/(MEH1/clay1)/Al device was $\sim 3 \times 10^{-5}$ cm^2 V^{-1} s^{-1}. This proves that, in our device, charge carriers are effectively confined in the quantum-well-like structure as depicted in the inset of Figure 5. Thus, the probability of exciton formation by bipolar recombination will increase. As mentioned previously, the formed excitons perform singlet decay efficiently without loosing the energy via a nonradiative decay. As a result, the EL efficiency drastically increases, as demonstrated in the inset of Figure 6.

Conclusion

Conjugated polymer/layered silicate nanocomposite material possesses high photostability due to its good gas barrier property. The PL from the nanocomposite film decayed with time more slowly than that of the pure MEH-PPV film. The composite film also showed a highly enhanced PL intensity. The LED prepared from the nanocomposite of MEH-PPV and organoclay possesses a high external quantum efficiency, 0.38% photons/electrons, with an Al cathode, which was enhanced by $\sim$100 times compared with that of the pure MEH-PPV device. Effective charge confinement of the composite, which was confirmed by the transient EL experiments, plays a critical role in improving the efficiency of the EL device. In addition, effective exciton confinement within this composite material occurs so that PL and EL efficiency would be greatly enhanced. In conclusion, the two-dimensional composite materials could be one of most effective candidates for polymer light-emitting devices with both high efficiency and good environmental stability.

Acknowledgment. This work was partially supported by Brain Korea 21 Project.

CM010201H